JOURNAL OF MECHANICAL ENGINEERING AND SCIENCES
ISSN: 2289-4659 e-ISSN: 2231-8380
VOLUME 17, ISSUE 2, 2023, 9492 – 9506
DOI: https://doi.org/10.15282/jmes.17.2.2023.8.0752

UNIVERSITI MALAYSIA PAHANG

RESEARCH ARTICLE

# Statistical analysis, modeling and multi-objective optimization of parameters intermittent turning process of AISI D3

**F. Khelfaoui, M. A. Yallese, N. Ouelaa, S. Chihaoui, S. Belhadi**

Laboratory of Mechanics and Structure (LMS), Department of Mechanical Engineering, University 8 May 1945, BP 401 Guelma 24000, Algeria
Phone: +213 37 10 05 53; Fax: + 213 37 10 05 55

**ABSTRACT -** Intermittent machining is characterized by its complex and irregular context. This intermittency causes machining to occur under difficult conditions that greatly influence the technological performance parameters. The aim of the present work is to evaluate the effects of input parameters, cutting speed, $V_c$, depth of cut, $a_p$, tool nose radius, r and feed rate, f, on surface roughness, $R_a$, tangential cutting force, $F_z$, motor power consumption, $P_m$, cutting power, $P_c$ and material removal rate (MRR), during intermittent turning (IT) of AISI D3 tool steel. Machining was performed with a triple CVD coated carbide tool ($Al_2O_3$/TiC/TiCN) by adopting a Taguchi L9 (3^4) experimental design. The ANOVA and RSM methods were used to analyze the effects of cutting factors on the outputs parameters resulting in statistical prediction models. In addition, a multi-objective optimization of the cutting conditions exploiting the desirability function (DF) was done according to four cases of relative importance corresponding to different industrial contexts. Furthermore, the grey relational analysis (GRA) method was applied and compared with the DF method. The results show that the optimal regime found by the DF method, (r =1.6mm, $V_c$= 240 m/min, f = 0.084 mm/rev and $a_p$ = 0.64 mm), favors $R_a$ and MRR. On the other hand, for the GRA method, the combination of (r = 0.4 mm, $V_c$ = 240 m/min f = 0.08 mm/rev and $a_p$ = 0.3 mm) favors the minimization of $F_z$, $P_m$ and $P_c$. This work presents an originality because the results found are very useful in the field of optimization for a better control of the process IT.

**ARTICLE HISTORY**
Received : 07th Dec. 2022
Revised : 23rd Mar. 2023
Accepted : 29th Mar. 2023
Published : 28th June 2023

**KEYWORDS**
*Intermittent turning*
*Machinability*
*Power consumption*
*Modelling*
*Optimization*

## 1.0 INTRODUCTION

The machining operation encompasses several different technological parameters, and the control of all of them is an industrial goal that depends on the context of machining, the machined material, and the number of factors studied [1, 2]. The discontinuous geometry of the part, the specific mechanical properties of the material, as well as its industrial destinations, impose additional difficulties on the manufacturer. Intermittent turning of materials is considered difficult machining, characterized by its complex and irregular context. This intermittent causes machining under severe conditions that greatly influence the technological performance parameters [3]. The exploitation of modeling and optimization methods is very effective for studying this kind of machining operation that can offer the desired interest to industrialists [4].

In this context of IT machining, several research works have been carried out. Ko et al. [5] conducted a study on the IT of bearing steel made of AISI 52100 to evaluate the performance of CBN cutting tools with different nitride contents. The output factors $V_B$, $R_a$, and $F_z$ were monitored. The results prove that increasing the nitride content induces a decrease in $R_a$ and $V_B$. Liu et al [6] performed experiments in IT of 2.25Cr1Mo0.25V steel with two different cutting tools of YT5 and GC4235. The obtained results showed that the tool performance GC4235 is superior to the tool YT5. Liu et al [7] conducted experiments in IT on 2.25Cr-1Mo-0.25V material with a coated carbide tool GC4235. Empirical models of MRR and $F_z$ parameters as a function of $V_c$, $a_p$, and f were proposed. Also, at low cutting speeds, abrasive wear and spalling were the main wear mechanisms; however, at high speeds, coating delamination and adhesive wear are prevalent. Carou et al [8] examined the effects of feed rate, MQ lubrication and type of workpiece interruption on vibration during Intermittent machining of UNS M11917 magnesium alloy using an uncoated carbide tool. F. Gong et al [9] conducted an experimental study in IT of 20CrMnTi hardened steel using $Al_2O_3$-TiC ceramic. The cutting forces and failure mechanisms of the cutting tools were evaluated as a function of varying cutting conditions. An experimental investigation was performed by Cui et al [10] to identify the optimal cutting parameters in the IT of AISI 1045 steel using an $Al_2O_3$/(W, Ti)C ceramic cutting tool. The results found allowed for an optimal area of surface roughness, cutting energy, and specific energy consumed using finite element method (FEM) as the optimization method.

Recently, Kudryashova et al. [11] conducted experimental study in IT, in order to understand the stabilization of cutting tools on complex surfaces. The analysis of the results showed that Ra is improved by 20% to 70% if a tool with a damping element in IT replaces the standard tool. In addition, Nayak et al. [12] performed a comparison between CT and

*CORRESPONDING AUTHOR | F. Khelfaoui | ✉ khel_fethi@yahoo.com

IT of AISI D6 tool steel using a tool with low CBN content. The results found in IT show that $V_c$ does not affect the cutting forces, and the wear mechanisms are abrasion and diffusion.

On the other hand, AISI D3 high-alloy steel has been the subject of several experimental studies that focus on machinability, MQ lubrication, tool wear, modeling, and optimization of cutting conditions [13-20]. Also, the desirability function approach is among the multi-objective optimization methods extensively used in many industrial sectors because of the advantages it presents [21-28]. Several researchers have adopted the GRA method as a multi-objective optimization method for cutting conditions due to its effectiveness in making the right decision for selecting the optimal parameters [29-35].

The review of the previous literature clearly shows that intermittent turning presents a case study frequently encountered in the industry, and this particular case of machining deserves special attention in order to evaluate, model, and optimize the technological performance parameters. Also, the particularity of this work lies in the fact that little investigation has been carried out on the intermittent turning of AISI D3 steel by considering the particular intermittent form on the workpiece and by considering four factors of input and four factors of output technical characteristics. Add to this, a comparison of the optimal cutting regimes obtained by two distinct optimization methods of DF and GRA.

The present work aims to evaluate the technological performance parameters namely $R_a$, $F_z$, $P_m$, $P_c$ and MRR as a function of cutting conditions r, $V_c$, $a_p$, and f of AISI D3 steel in IT context. ANOVA was used to quantify the influence of input factors on the responses. The statistical treatment of the results allowed us to propose prediction models in IT. Two multi-objective optimization methods were performed by exploiting the DF and GRA approaches according to objectives frequently found in the industry. The results found are of primary importance to researchers working on multi-objective optimization problems of operating factors during intermittent machining.

## 2.0 EXPERIMENTAL PROCEDURE

### 2.1 Machined Material and Cutting Tool

The material of study is high-alloy steel AISI D3, intended for cold work with a very high resistance to abrasive wear, medium toughness, dimensional stability, and high resistance to compression. This material has a wide application in the industrial field, such as in machining and forming tools such as punches, and rolling mills, as well as the manufacture of measuring instruments such as gauges, stamps, and gauges [25]. The chemical composition of AISI D3 steel is shown in Table 1. The workpiece used in turning tests is 185 mm in length and 70 mm in diameter. In order to ensure intermittent turning us made three bearings over a length of 85 mm, the width of the groove is 3.33 mm. A cutting insert composed of eight cutting edges made of triple-coated metal carbide ($Al_2O_3$/TiC/TiCN) of the Sandvik brand GC4215 was used for IT tests as shown in Figure 1. It is mounted on a tool holder on ISO designation PSBNR 2525M12 with geometry represented by $\gamma=-6°$, $\lambda=-6°$, $\alpha=6°$, and $\chi r=75°$. For each machining operation, the cutting tool undergoes three (3) shocks successively.

Table 1. Chemical composition of AISI D3 steel

| Composition | C | Si | Ni | Mo | Mn | S | P | Cu | Cr |
|---|---|---|---|---|---|---|---|---|---|
| Percentage (%) | 2 | 0.31 | 0.259 | 0.124 | 0.29 | 0.009 | 0.011 | 0.162 | 12 |

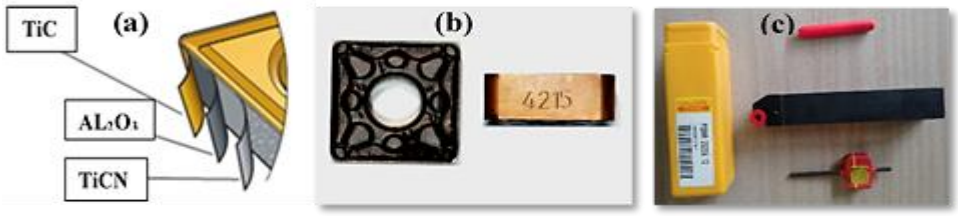


Figure 1. Cutting tool; (a) coating layer, (b) cutting insert and (c) tool holder

### 2.2 Measuring Devices and Experimental Design

Intermittent turning experiments were performed on a Tos Trencin SN40C brand lathe with 6.6 kW of power, following the standard ISO 3685. The lathe is equipped with a variable speed drive, model ABB series ACS355, with a speed sensor allowing the control of spindle speed. The value of the $R_a$ criterion was measured with a roughness tester model MITUTOYO SJ-210 as shown in Figure 2(a), 2(b) and 2(c). It consists of a 5-µm diamond tip feeler that moves axially over a distance of 4 mm with a cut-off $\lambda$= 0.8 mm on the machined surface. The measurement is repeated three times, following an angular position of 120° for each test. The tangential cutting force $F_z$, was recorded in real time using a Kistler dynamometer type 9257 B, as can be seen in Figure 2(d), 2(e) and 2(f). Figures 2(g), 2(h) and 2(i) show the measurement of motor power consumption, $P_m$ using a LUTRON DW-6095 three-phase power analyzer in real time throughout the intermittent machining operation. The entire experimental procedure is shown in Figure 2. In order to

investigate the influence of the selected input parameters on the targeted response parameters, a L9 (3^4) Taguchi experimental design was chosen to reduce the cost of the experiments and simplify the experimental protocol. The operating conditions chosen to perform the experiments and the values of the cutting parameters are organized in Tables 2 and 3.

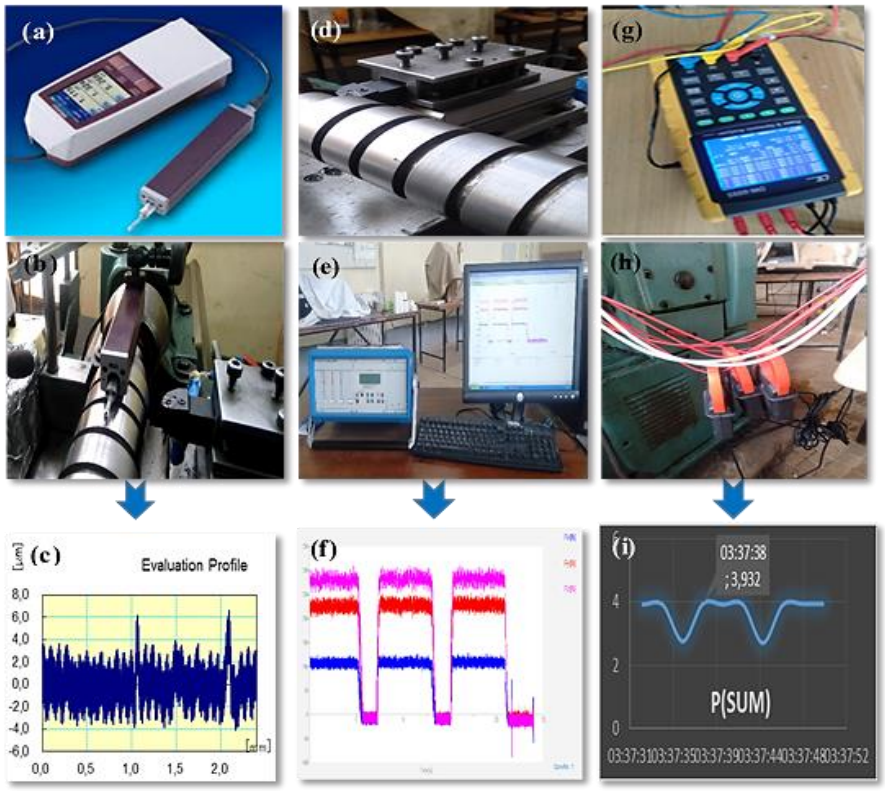


Figure 2. Equipment and materials

Table 2. Operational conditions

| Elements | Description |
|---|---|
| Lathe | SN40C (6.6 kW) |
| Workpiece | AISI D3 |
| Cutting tool | $AI_20_3$/TiC /TiNC Carbide insert (CVD) |
| Tool holder | SANDVIK PSBNR 2525M 12 |

Table 3. Cutting conditions

| Elements | Description | Values |
|---|---|---|
| Input parameters | Cutting speed ($V_c$) | 240 ; 280 ; 320 (m/min) |
| | Feed rate (f) | 0.08 ; 0.12 ; 0.16 (mm/rev) |
| | Depth of cut ($a_p$) | 0.3 ; 0.6 ; 0.9 (mm) |
| | Nose raduis (r) | 0.4 ; 1.2 ; 1.6 (mm) |
| Output parameters | $R_a$ ; $F_z$ ; $P_m$ ; $P_c$ ; MRR | - |
| Cutting procedure | Intermittent turning | - |
| Lubrication | Dry | - |

### 2.3 Cutting Power and Material Removal Rate

The cutting power consumed, $P_c$ in the machining operations, is a very important indicator to follow, because of its impact on the final cost of a product [36]. This indicator deserves to be evaluated in order to minimize it in the optimization studies. In our case the $P_c$, is calculated according to Eq. (1) based on the measured value of the $F_z$.

$$P_c = \frac{F_Z \times V_C}{60} \text{ (Watt)} \quad (1)$$

The material removal rate, MRR is a factor that represents productivity [37]. Which calculated by following equation.

$$MRR = \frac{V_c \times a_p \times f \times 10^3}{60} \quad (mm^3/s) \tag{2}$$

## 3.0 RESULTS AND DISCUSSION

### 3.1 Experimental Results

The results of the tests performed according to the Taguchi L9 design (3^4) are collected and organized in Table 4. These results obtained represent the response parameters: $R_a$, $F_z$, $P_m$, $P_c$, and MRR as a function of the input parameters r, $V_c$, $a_p$, and f. It appears from the results that the $R_a$ varies from 0.825 µm to 1.201 µm. $F_z$ varies between 42.23 N and 240.45 N; $P_m$ varies from 2900 to 4900 Watt. $P_c$ varies between 168.92 Watt and 1282.40 Watt and finally the MRR varies from 96 $mm^3/s$ to 768 $mm^3/s$. Figure 3 shows the profile of the cutting forces components in IT. The $F_z$ component has been considered in this work because it is preponderant than $F_x$ and $F_y$. Figure 4 shows the $P_m$ profile during intermittent turning.

Table 4. Experimental results

| | Input Factors | | | | | | Responses | | |
|---|---|---|---|---|---|---|---|---|---|
| N° | r (mm) | $V_c$ (m/min) | f (mm/rev) | $a_p$ (mm) | $R_a$ (µm) | $F_z$ (N) | $P_m$ (Watt) | $P_c$ (Watt) | MRR ($mm^3/s$) |
| 1 | 0.4 | 240 | 0.08 | 0.3 | 0.867 | 42.23 | 2900 | 168.92 | 96 |
| 2 | 0.4 | 280 | 0.12 | 0.6 | 1.034 | 145.69 | 3652 | 679.89 | 336 |
| 3 | 0.4 | 320 | 0.16 | 0.9 | 1.201 | 240.45 | 4900 | 1282.40 | 768 |
| 4 | 1.2 | 240 | 0.12 | 0.9 | 0.934 | 155.85 | 3912 | 623.40 | 432 |
| 5 | 1.2 | 280 | 0.16 | 0.3 | 1.060 | 142.36 | 3804 | 664.35 | 224 |
| 6 | 1.2 | 320 | 0.08 | 0.6 | 0.873 | 145.25 | 4120 | 774.67 | 256 |
| 7 | 1.6 | 240 | 0.16 | 0.6 | 0.938 | 178.19 | 3932 | 712.76 | 384 |
| 8 | 1.6 | 280 | 0.08 | 0.9 | 0.825 | 162.53 | 4355 | 758.47 | 336 |
| 9 | 1.6 | 320 | 0.12 | 0.3 | 0.878 | 110.62 | 4100 | 589.97 | 192 |

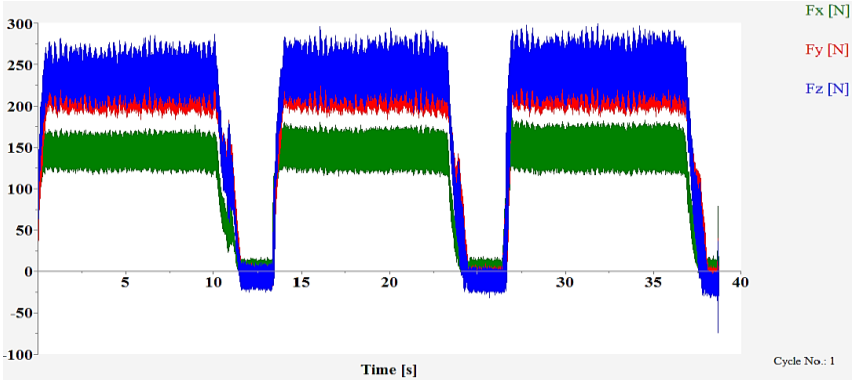


Figure 3. Cutting forces profile in IT

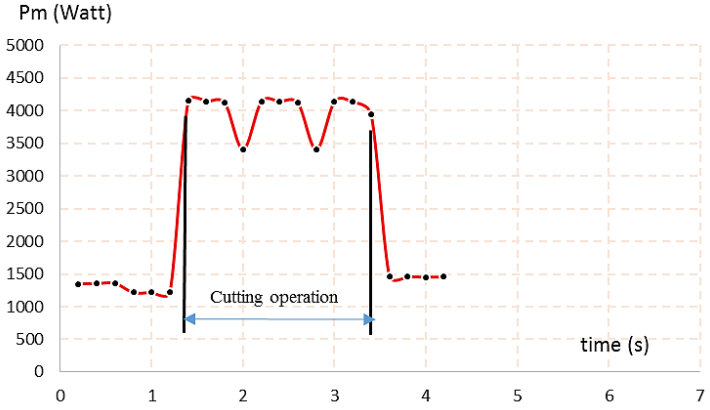


Figure 4. Motor power profile in IT

### 3.2 ANOVA of Performances

ANOVA results of $R_a$, $F_z$, $P_m$ and $P_c$ responses are exposed in Table 5. The abbreviations for the values reported in Table 4 are, Dof is degrees of freedom, SumSqr is sum of squares, Cont % is percentage contribution of each factor, SumSq adjusted is adjusted sum of squares; MS adjusted is adjusted mean squares. F is the Fisher value and p is the probability value. If the value of p is less than 0.05, the input parameter is considered significant [38]. Surface roughness ANOVA results reveal that the two input parameters f and r possess a great influence with cont% of 57.86% and 29.63% respectively, followed by $V_c$ with a cont% of 6.53%, however $a_p$ is non-significant with a cont% of 3.46%. These results are in agreement with those of D. Carou et al. [39]. $a_p$ and f, are the main factors having the greatest influence on $F_z$, their cont% is 51.82% and 33.19% respectively. The $V_c$ factor comes in third place with a cont% of 10.75%, while r is non-significant $P > 0.05$ with a cont% of 0.41%. Gong et al [9] reported similar results, Cui et al. [40], Ni et al [41] indicating that the increase of both factors $a_p$ and f causes the increase of effort $F_z$. From the ANOVA of $P_m$, it is obvious that all the input factors are significant; $V_c$ and $a_p$ have the major influence, with a cont% of 40.37% and 39.93% respectively. They are followed by f and r, which have cont% of 11.37% and of 5.79% respectively. The results of $P_c$ indicate that the factors $V_c$, f and $a_p$ are significant, with cont% of 39.50%, 33.45% and 23.51% respectively. However, the r is insignificant with a contribution of 0.15%. A comparable study by Safi et al [25] indicated that the factors $V_c$ and $a_p$ are the first responsible factors on the increase of $P_c$. For the ANOVA of the MRR, it has not been treated, since it is a parameter calculated by equation no. 2 as a function of the input factors. This equation will be exploited in the optimization study.

Figure 5 summarizes the contribution of each cutting factor on the response parameters, and ANOVA error. It is clear from this figure that $a_p$ is the factor with the most significant effect on the three parameters $F_z$, $P_m$ and $P_c$ with contributions that exceed the value of 39%, while for the parameter $R_a$, the factor f has the greatest dominance with a contribution of over 57%. Figure 6 plots the main effects of the output parameters $R_a$, $F_z$, $P_m$, and $P_c$ as a function of variations in the input factors r, $V_c$, f, and $a_p$. The factor with the largest slope has the greatest influence on the output parameter under study; the figure confirms that $a_p$ has a strong signification on $F_z$, $P_m$ and $P_c$. Also, $V_c$ and f have impact on all output parameters under study. Finally, the factor r particularly has the largest slope on the graph $R_a$, compared to the other output parameters.

Table 5. ANOVA of Ra, Fz, Pm and Pc

| Source | Dof | Sum sqr | Cont % | Sumsqr adjusted | MS adjusted | F value | p value |
|---|---|---|---|---|---|---|---|
| | | | | ($R_a$) | | | |
| r | 1 | 0.034304 | 29.63% | 0.034304 | 0.034304 | 46.96 | 0.002 |
| $V_c$ | 1 | 0.007562 | 6.53% | 0.007561 | 0.007561 | 10.35 | 0.032 |
| f | 1 | 0.066993 | 57.86% | 0.066993 | 0.066993 | 91.70 | 0.001 |
| $a_p$ | 1 | 0.004004 | 3.46% | 0.004004 | 0.004004 | 5.48 | 0.079 |
| Error | 4 | 0.002922 | 2.52% | 0.002922 | 0.000731 | | |
| Total | 8 | 0.115784 | 100.00% | | | | |
| | | | | ($F_z$) | | | |
| r | 1 | 90.8 | 0.41% | 90.8 | 90.8 | 0.42 | 0.551 |
| $V_c$ | 1 | 2402.0 | 10.75% | 2402.0 | 2402.0 | 11.21 | 0.029 |
| f | 1 | 7419.5 | 33.19% | 7419.5 | 7419.5 | 34.63 | 0.004 |
| $a_p$ | 1 | 11582.6 | 51.82% | 11582.6 | 11582.6 | 54.07 | 0.002 |
| Error | 4 | 856.9 | 3.83% | 856.9 | 214.2 | | |
| Total | 8 | 22351.8 | 100.00% | | | | |
| | | | | ($P_m$) | | | |
| r | 1 | 134979 | 5.79% | 134979 | 134979 | 9.14 | 0.039 |
| $V_c$ | 1 | 940896 | 40.37% | 940896 | 940896 | 63.73 | 0.001 |
| f | 1 | 265020 | 11.37% | 265020 | 265020 | 17.95 | 0.013 |
| $a_p$ | 1 | 930628 | 39.93% | 930628 | 930628 | 63.04 | 0.001 |
| Error | 4 | 59053 | 2.53% | 59053 | 14763 | | |
| Total | 8 | 2330577 | 100.00% | | | | |
| | | | | ($P_c$) | | | |
| r | 1 | 966 | 0.15% | 966 | 966 | 0.18 | 0.697 |
| $V_c$ | 1 | 217345 | 33.45% | 217345 | 217345 | 39.47 | 0.003 |
| f | 1 | 152784 | 23.51% | 152784 | 152784 | 27.75 | 0.006 |
| $a_p$ | 1 | 256694 | 39.50% | 256694 | 256694 | 46.62 | 0.002 |
| Error | 4 | 22026 | 3.39% | 22026 | 5507 | | |
| Total | 8 | 649815 | 100.00% | | | | |

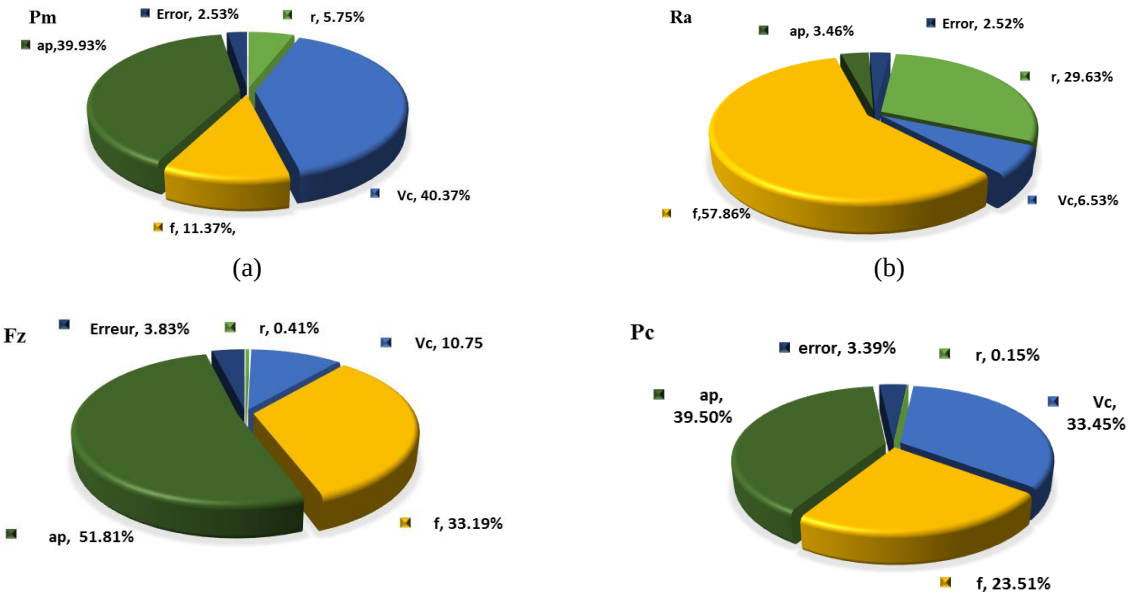


Figure 5. Input factor contribution: (a) Pm, (b) Ra, (c) Fz and (d) Pc

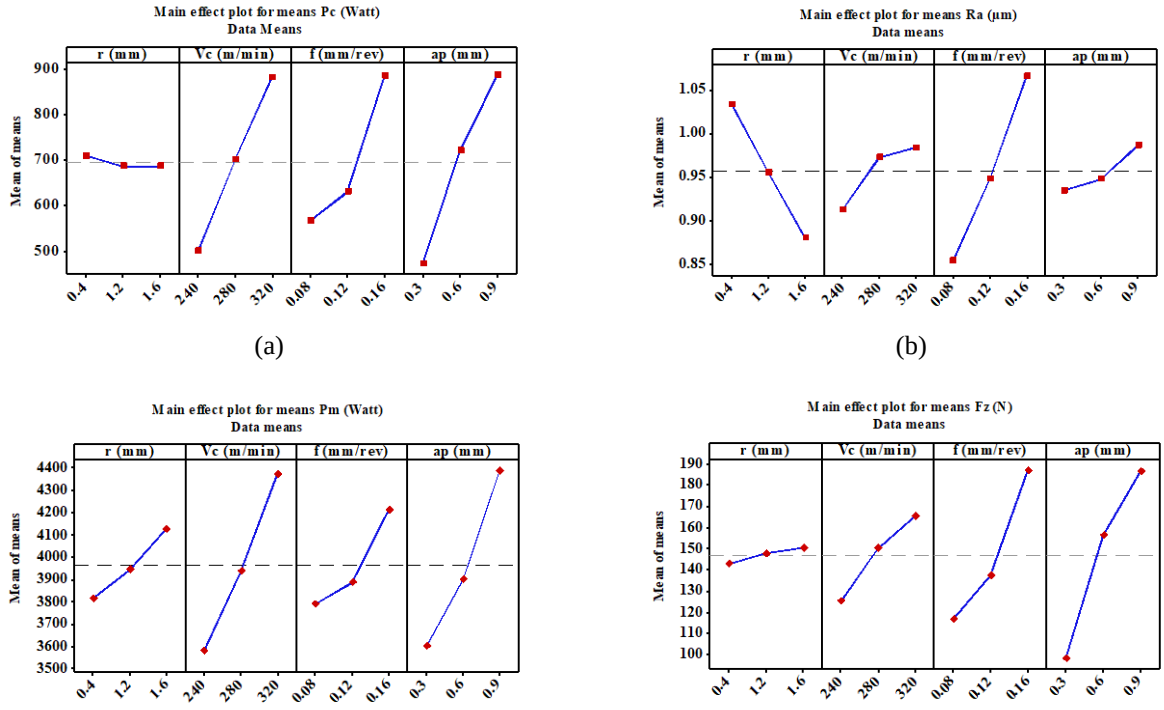


Figure 6. Main effects graphs for: (a) Pc, (b) Ra, (c) Pm and (d) Fz

### 3.3 Response Modelling

Modeling the output parameters of a technological process presents an important task because it allows prediction [42]. Generally, the prediction models found are of significant interest in the optimization stage of cutting conditions [43], [44]. In our case study, the relationship between the output responses and the input factors was established by linear regression equations, presented as mathematical models Eq. (3) to Eq. (6) with a different $R^2$.

$$R_a = 0.4715 - 0.1238\ r + 0.000888\ V_c + 2.642\ f + 0.0861 a_p \qquad (R^2 = 97.48) \qquad (3)$$

$$F_z = -193.2 + 146.5\ a_p + 879\ f + 0.500\ V_c + 6.37 r \qquad (R^2 = 96.1) \qquad (4)$$

$$P_m = -488 + 245.5\ r + 9.90\ V_c + 5254\ f + 1313\ a_p \qquad (R^2 = 97.47) \qquad (5)$$

$$P_c = -1508 - 20.8\ r + 4.758\ V_c + 3989\ f + 689\ a_p \qquad (R^2 = 96.61) \qquad (6)$$

Eq. (3) to Eq. (6) have been exploited to plot the response surfaces 3D as well as the contours for the studied response parameters, taking into account the two most influential input parameters, illustrated in Figure 7. In addition, the contour plots represent a capital interest because they allow one to estimate the value of the studied output parameter according to the combination of the two chosen input factors [45].

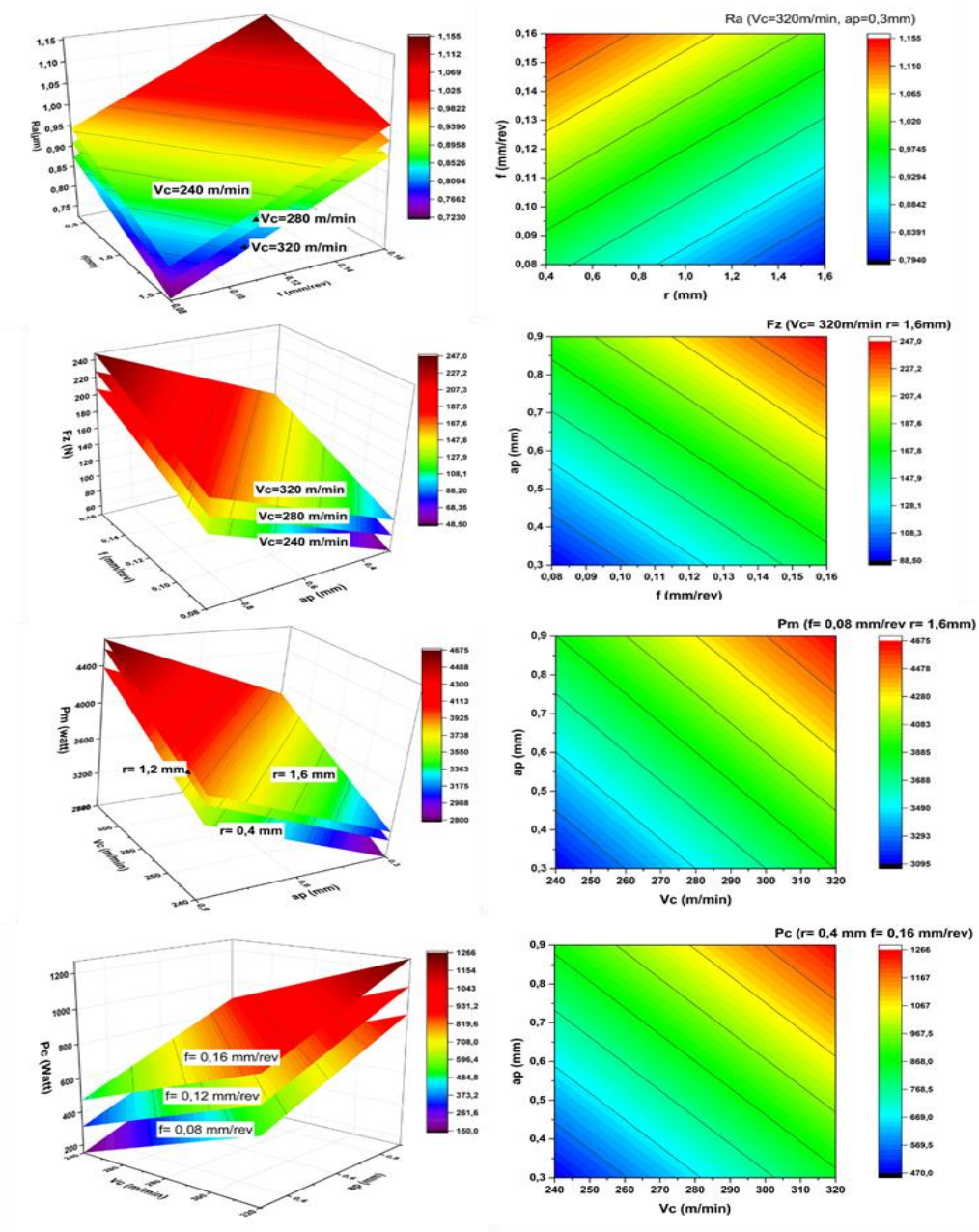


Figure 7. 3D Graphs and contours of Ra, Fz, Pm and Pc

The studied performances $R_a$, $F_z$, $P_m$, and $P_c$ are represented by graphs of the response surfaces and contours according to the two most influential input parameters. The reading of the response surface and contour graphs clearly shows that an increase of f causes a degradation of the machined surface quality translated by the increase of the quality index Ra, because the increase of feed rate creates helical grooves due to the translational movement of the cutting tool and the rotation of the workpiece simultaneously. The larger f is, the wider and deeper the helical grooves became. However, increasing r leads to an improvement in surface quality. This is due to the smoothing phenomenon of the machined surface that occurs when r increases. As the depth of cut increases, the cutting surface in contact with the tool also increases, which increases the force required to cut the material. This results in an increase in $F_z$. Therefore, an increase in feed rate per revolution f results in an increase in cutting force, $F_z$, this is because f is directly related to the amount of material the tool must remove MRR. An increase in f means that the tool must remove more material, which results in an increase in cutting force, $F_z$. It is obvious that an increase in cutting speed leads to an increase in cutting power, $P_c$. The same way the increase of $a_p$ causes the increase of $P_c$ because the power is directly related to the cutting force, which is justified in our case where the increase of $a_p$ induces an increase of $F_z$, and this increase of $F_z$ generates in parallel an increase of $P_c$.

Moreover, as long as $P_c$ is part of the power of the engine $P_m$, this imperatively induces that any increase of the power, $P_c$ necessarily causes an increase of $P_m$.

### 3.4 Multi-Objective Optimization

Due to the severe competition and rivalry in the global market between mechanical manufacturing companies. Also, to meet the requirements of customers in terms of quality, productivity and final cost of the product, multi-objective optimization of performance parameters has become a primary objective of several researchers [45]. In this work, we have exploited two approaches; DF approach based on the mathematical models found and GRA which is part of MCDM method family. The goal is to propose one or more optimal cutting combinations of cutting parameters according to the different desired objectives. We point out here that the comparison between the two approaches DF and GRA was limited only to the case where all the output parameters have the same importance.

#### 3.4.1 Desirability function

The method is widely used in solving multi-objective optimization problems because of its simplicity and effectiveness in putting in the hands of the users the best solutions for choosing the cutting parameters that ensure the global objective aimed at. DF with the value closest to 1 indicates the optimal combination of cutting parameters [46]. It is given by the following equations:

$$\text{Des(y)}=\begin{cases} 0 & y < Low \\ \left(\frac{y-Low}{Tar-Low}\right)^{w} & Low \le y \le Tar \\ 1 & y > Tar \end{cases} \quad (7)$$

$$\text{Des(y)}=\begin{cases} 1 & y < Tar \\ \left(\frac{Up-y}{UP-Tar}\right)^{w} & Tar \le y \le Up \\ 0 & y > Up \end{cases} \quad (8)$$

$$\text{Des}_{comb}= (Des1\ x\ Des2\ x\ \dots x\ Desi\ x\ \dots x\ Desn)^{\frac{1}{n}} =(\prod_{i=1}^{n} Des_i)^{\frac{1}{n}} \quad (9)$$

In this study, four optimization cases favoring the choice of optimal cutting conditions during intermittent machining of AISI D3 are considered. In Table 6, the constraints of the optimization, the desired objectives as well as the importance chosen for the output parameters, which varies from 1 to 5 according to fourth studied cases, are recorded.

Table 6. Optimization constraints and importance

| | Parameters | Values (V) | | Objective | Importance | | | |
|---|---|---|---|---|---|---|---|---|
| | | *(p) Lower* | *(p) Upper* | | *1st Case* | *2nd Case* | *3rd Case* | *4th Case* |
| Input | r | 0.4 | 1.6 | *low*≤ V ≤ *up* | - | - | - | - |
| | $V_c$ | 240 | 320 | | - | - | - | - |
| | f | 0.08 | 0.16 | | - | - | - | - |
| | $a_p$ | 0.3 | 0.9 | | - | - | - | - |
| Output | $R_a$ | 0.825 | 1.201 | Minimize | 5 | 5 | 5 | 5 |
| | $F_z$ | 42.23 | 240.45 | Minimize | 1 | 1 | 5 | 1 |
| | $P_m$ | 2900 | 4900 | Minimize | 1 | 5 | 5 | 1 |
| | $P_c$ | 168.92 | 1282.40 | Minimize | 1 | 1 | 5 | 1 |
| | MRR | 96 | 768 | Maximize | 1 | 5 | 5 | 5 |

Table 7 shows the final solutions obtained by DF approach. These solutions include the optimal cutting regime, the corresponding optimized outputs, and the desirability value for the four optimization cases considered. These found solutions meet the manufacturers' objectives during the machining operation of IT parts made of D3 steel. In the first optimization case, $R_a$ takes the maximum value of importance of 5; on the other hand, the other parameters take a minimum importance of 1. The objective is to have an excellent surface finish that meets the requirements of a customer who prefers first-order surface quality [47]. This is a finishing operation, where $R_a$ must be minimized. The optimal regime that corresponds to this machining operation is shown in Table 7 with a minimum roughness $R_a$ equal to 0.825 µm and a desirability of 0.754. The second optimization case considers a maximum importance of (5) attributed to the three performance parameters $R_a$, $P_m$ and MRR, however $F_z$ and $P_c$ take a minimum importance equal to 1. This optimization case is interesting in the case of mass production, when the desired objective is to seek a compromise between minimizing $R_a$, $P_m$ and maximizing productivity. The optimized output parameters take the values 0.887 µm, 3665.08 Watt, and 309.145 $mm^3/s$ for $R_a$, $P_m$, and MRR respectively, with a desirability of 0.556. For the third

optimization case, an importance of 5 is assigned to the five performance parameters in order to minimize $R_a$, $F_z$, $P_m$, $P_c$ and maximize the MRR. A trade-off between all outputs is sought in this optimization case. The optimal regime is proposed in Table 7 with a found desirability of 0.603. The fourth optimization case aims at maximum productivity and surface quality simultaneously [48]. An importance of 5 is assigned to the parameters $R_a$ and MRR, while an importance of 1 is assigned to the remaining parameters. This case study is interesting for a customer who is only interested in quality and productivity while energy consumption is in last order. The optimized outputs take the values 0.908 µm and 404.918 $mm^3/s$ for $R_a$ and MRR respectively, with a desirability of 0.560.

In conclusion, we can say that the choice of an optimal cutting speed in the context of intermittent machining depends on the objective. Either the search for maximum surface quality, maximum productivity, minimum energy consumption, minimum production cost of machined parts or also, the combination of one, two or all the objectives together [23, 49-51].

Table 7. Selected solutions

| | Input factors | | | | Output parameters | | | | | Des |
|---|---|---|---|---|---|---|---|---|---|---|
| | r | $V_c$ | $a_p$ | f | $R_a$ | $F_z$ | $P_m$ | $P_c$ | MRR | |
| 1st case | 1.6 | 240 | 0.57 | 0.087 | 0.825 | 91.50 | 3359.08 | 310.94 | 200.59 | 0.754 |
| 2nd case | 1.6 | 240 | 0.71 | 0.109 | 0.887 | 130.99 | 3665.08 | 494.12 | 309.15 | 0.556 |
| 3rd case | 1.6 | 240 | 0.64 | 0.084 | 0.846 | 95.98 | 3376.43 | 330.74 | 216.01 | 0.603 |
| 4th case | 1.6 | 240 | 0.71 | 0.143 | 0.908 | 168.53 | 4003.51 | 670.97 | 404.92 | 0.56 |

### 3.4.2 GRA method

The GRA method belongs to the family of methods MCDM [52], it is suitable for solving multi-objective problems. In our case it is applied for the optimization of cutting conditions in intermittent machining with the aim of maximizing the MRR and minimizing the performance parameters $R_a$, $F_z$, $P_m$ and $P_c$ simultaneously. The GRA method is based on the steps illustrated in Figure 8. In this study, the operation of GRA method is performed by setting the same objectives as the third optimization case studied by DF, which is interested in optimizing the five performance parameters simultaneously with equal importance. Hereunder the GRA steps, the equations used for the calculations, and the meanings of each term in the equations [53]. The results obtained are organized in Table 8.

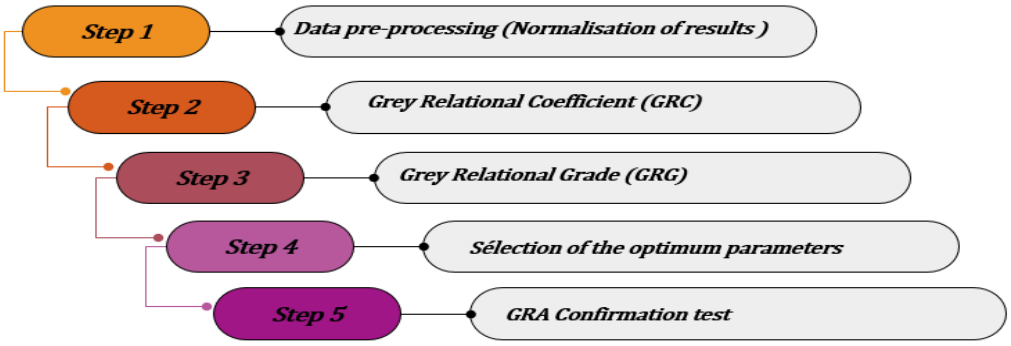


Figure 8. Steps of GRA method

**Step 1: Normalization of results**

$$x_i(k) = \frac{max\left(x_i^0(k)\right) - x_i^0(k)}{max\left(x_i^0(k)\right) - min\left(x_i^0(k)\right)} \quad \text{Lower is better} \tag{10}$$

$$x_i(k) = \frac{x_i^0(k) - min\left(x_i^0(k)\right)}{max\left(x_i^0(k)\right) - min\left(x_i^0(k)\right)} \quad \text{Greater is better} \tag{11}$$

where, $x_i(k)$ : normalized value;$x_i^0(k)$: result value; $max\left(x_i^0(k)\right)$:max value of ($k^{th}$) response $x_i^0(k)$ $min\left(x_i^0(k)\right)$: min value of ($k^{th}$) response $x_i^0(k)$.

**Step 2: Grey relational coefficient (GRC)**

$$GRC = \frac{\Delta_{min} + \beta\Delta_{max}}{\Delta_{0i} + \beta\Delta_{max}} \tag{12}$$

$$\Delta_{0i}(k) = \|x_0(k) - x_i(k)\| \tag{13}$$

where, $\Delta_{0i}$ (k): deviation sequence, difference in absolute value between $x_0^k$ (k) and $x_i^k$ (k)

$\Delta_{min}$: The lowest value of $\Delta_{0i}$ $(k)$; $\Delta_{max}$: the highest value of $\Delta_{0i}$ $(k)$

$\beta$: Identification coefficient defined in the range $0 \leq \beta \leq 1$ in our case, the value of $\beta$ is 0.5.

**Step 3: Grey relational grade (GRG)**

$$GRG = \frac{1}{n}\sum_{k=1}^{n} GRC \tag{14}$$

where, n: is the number of tests.

**Step 4: Selection of the optimum parameters**

Classification of grg values in descending order, the largest grg value has the best range of optimal parameters.

**Step 5: GRA confirmation test**

$$\gamma_i = \gamma_m + \sum_{i=1}^{p} (\overline{\gamma_i} - \gamma_m) \tag{15}$$

where, $\gamma_m$ : is the total mean grg; $\overline{\gamma_i}$ : is the mean grg at the optimal level; p: is the number of major variables.

Table 8 shows the coefficients and ranks of the Gray Relation for each experiment in the Taguchi L9 design. Applying the instructions in step 4, it is clearly observed that the trial number 1 has the largest GRG value of 0.830, the optimal regime proposed by this method is that of experiment number 1: r = 0.4 mm, $V_c$ = 240 m/min, f = 0.08mm/rev, $a_p$ = 0.3 mm. The Figure 9 presents the graph of the main effects of GRG according to the variations of the input factors r, $V_c$, f and $a_p$. Table 9 shows the responses of GRG averages, the factor with largest Delta value has greatest influence on GRG.

Table 8. GRC and GRG results

| No. Exp | GRC | | | | | GRG | Rank |
|---|---|---|---|---|---|---|---|
| | $R_a$ | $F_z$ | $P_m$ | $P_c$ | MRR | | |
| 1 | 0.817 | 1.000 | 1.000 | 1.000 | 0.333 | 0.830 | 1 |
| 2 | 0.474 | 0.489 | 0.571 | 0.521 | 0.438 | 0.499 | 7 |
| 3 | 0.333 | 0.333 | 0.333 | 0.333 | 1.000 | 0.467 | 9 |
| 4 | 0.633 | 0.466 | 0.497 | 0.551 | 0.500 | 0.529 | 4 |
| 5 | 0.444 | 0.497 | 0.525 | 0.529 | 0.382 | 0.476 | 8 |
| 6 | 0.797 | 0.490 | 0.450 | 0.479 | 0.396 | 0.523 | 5 |
| 7 | 0.625 | 0.422 | 0.492 | 0.506 | 0.467 | 0.502 | 6 |
| 8 | 1.000 | 0.452 | 0.407 | 0.486 | 0.438 | 0.556 | 2 |
| 9 | 0.780 | 0.592 | 0.455 | 0.569 | 0.368 | 0.553 | 3 |

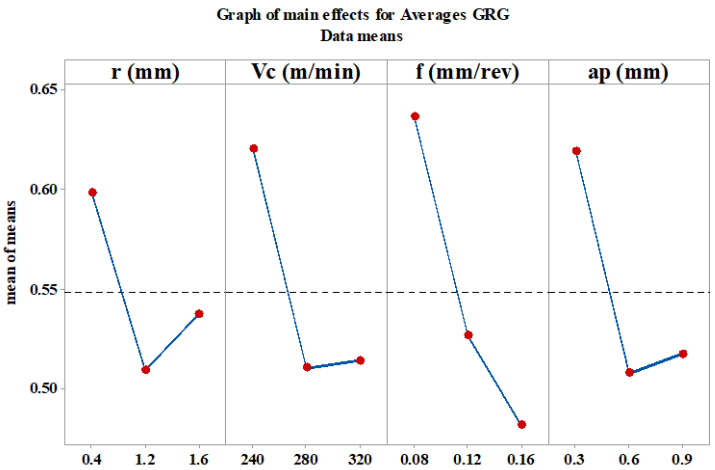


Figure 9. Main effects graphs for Averages GRG

Table 9. Responses for GRG

| Parameters | GRG | | | Delta Max-Min | Rank |
|---|---|---|---|---|---|
| | Level 1 | Level 2 | Level 3 | | |
| r | 0.5984 | 0.5091 | 0.5371 | 0.0893 | 4 |
| $V_c$ | 0.6205 | 0.5102 | 0.5140 | 0.1104 | 3 |
| f | 0.6364 | 0.5269 | 0.4815 | 0.1549 | 1 |
| $a_p$ | 0.6195 | 0.5077 | 0.5175 | 0.1118 | 2 |

### 3.4.3 Comparison between DF and GRA Optimization

The results obtained with the two multi-objective optimization methods are summarized in Table 10. The purpose of this comparison is to establish the performance of each method and to leave the choice to the industrialists to decide the application of this or that approach. It is clear that the DF favors the parameters of surface quality and productivity at the same time, where the roughness is minimal, and productivity is maximal $R_a$ =0.846µm and MRR=216.01mm$^3$/s. On the other hand, the factors $F_z$, $P_m$, and $P_c$ take maximum values. On the other hand, the GRA proposes an optimal regime favoring the minimization of cutting force $F_z$ by a percentage of 56.00% compared to the DF, as well as a minimization of energy consumption of 14.11% and 48.93% for $P_m$ and $P_c$ respectively. The surface quality value $R_a$=0.867µm found is almost comparable to that found by DF with a small increase of 2.48% only, however the productivity parameter is very low MRR=96 mm$^3$/s which is a strong decrease of 55.56% compared to DF. Finally, both methods propose to the industrialists two optimal regimes with the same cutting speed $V_c$ = 240 m/min, and almost the same feed rate f=0.08 mm/rev while the two factors r and $a_p$ are totally different.

Table 10. Results of DF and GRA methods

| | Input factors | | | | Output parameters | | | | |
|---|---|---|---|---|---|---|---|---|---|
| | r (mm) | $V_c$ (m/min) | f (mm/rev) | $a_p$ (mm) | $R_a$ (µm) | $F_z$ (N) | $P_m$ (Watt) | $P_c$ Watt) | MRR (mm$^3$/s) |
| DF | 1.6 | 240 | 0.084 | 0.64 | 0.846 | 95.98 | 3376.43 | 330.74 | 216.01 |
| GRA | 0.4 | 240 | 0.08 | 0.3 | 0.867 | 42.23 | 2900 | 168.92 | 96 |
| Difference (%) | -75.00 | 0.00 | -4.76 | -53.05 | 2.48 | -56.00 | -14.11 | -48.93 | -55.56 |

## 3.5 Relationship between Motor Power and Cutting Power

For the realized experimental design, the change of the cutting conditions for different tests generates different values of $P_c$ and $P_m$. Figure 10 shows the histogram of the recorded values of $P_c$ and $P_m$. The ratios $(P_m/P_c)$ for the 9 tests performed are as follows: {17.17; 5.37; 3.82; 6.28;5.73; 5.32; 5.52; 5.74; 6.95}. The power $P_c$ is included in the total power consumed by the motor $P_m$. Figure 11 shows the histogram of the percentages of $P_c$ versus $(P_m - P_c)$ for each test performed.

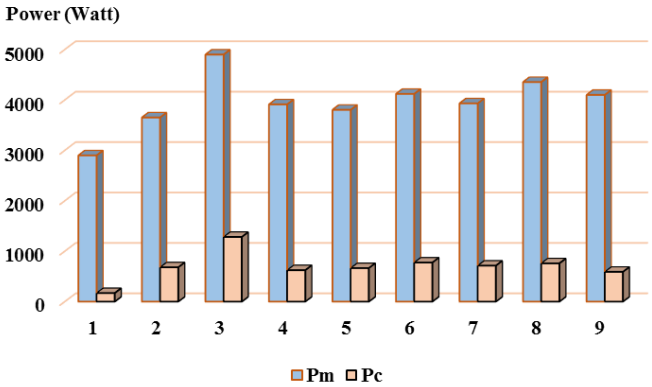


Figure 10. $P_m$ and $P_c$ for each test

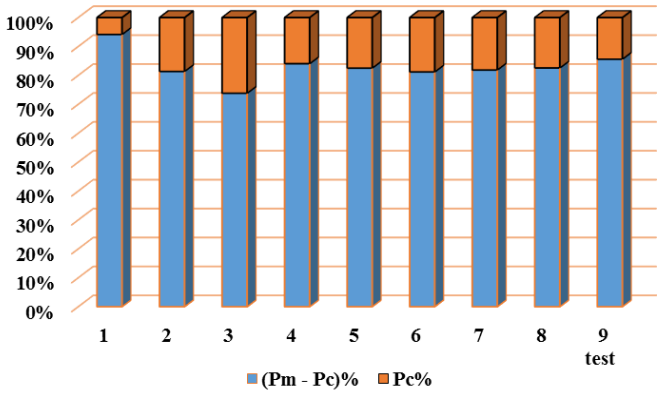


Figure 11. Rate of $P_c$ and $P_m$-$P_c$

## 4.0 CONCLUSION

The present work concerns an experimental study of modeling and multi-objective optimization of cutting parameters during intermittent machining of AISI D3 steel using DF and GRA methods. The results of the ANOVA of $R_a$ show that the factors f and r have the greatest impact on $R_a$, while the ANOVA of $F_z$ reveals that $a_p$ and f have the greatest influence. However, the ANOVA of Pm and $P_c$ clearly shows that $V_c$ and $a_p$ are the most dominant factors. In addition, the mathematical models found for $R_a$, $F_z$, $P_m$ and $P_c$ in the context of intermittent turning are accurate, with high $R^2$ ranging from 96.1% to 97.48%. These models are very useful for prediction and optimization.

Multi-objective optimization of cutting conditions by applying the DF method to four well-defined cases, which meet industrial requirements, offers the possibility of choosing the optimum solution according to the desired case. The comparison of the optimal regimes found by the DF and GRA methods is of great industrial interest, as it enables the correct selection of the optimal regimes that correspond to the targeted objectives. The DF method gives the best results for minimizing $R_a$ and maximizing MRR. The GRA method, on the other hand, favours minimization of $F_z$, $P_m$ and $P_c$, while maintaining surface quality very close to that of the DF method.

## 5.0 ACKNOWLEDGEMENT

The present research was undertaken by the “Metal Cutting Research Group” of the (LMS) Laboratory of the 8 May 1945-Guelma University, Algeria. The work is funded by LMS Laboratory of the 8 May 1945-Guelma University, Algeria and (DGRSDT) under the PRFU research projects A11N01UN240120220002-A11N01UN240120230001.

## 6.0 REFERENCES

[1] D. Carou, E. M. Rubio, C. H. Lauro, L. C. Brandão, and J. P. Davim, "Study based on sound monitoring as a means for superficial quality control in intermittent turning of magnesium workpieces," *Procedia CIRP*, vol. 62, pp. 262-268, 2017.

[2] E. M. Rubio, M. Villeta, B. de Agustina, and D. Carou, "Surface roughness analysis of magnesium pieces obtained by intermittent turning," in *Materials Science Forum*, vol. 773, pp. 377-391, 2014.

[3] X. Cui and J. Guo, "Identification of the optimum cutting parameters in intermittent hard turning with specific cutting energy, damage equivalent stress, and surface roughness considered," *The International Journal of Advanced Manufacturing Technology*, vol. 96, pp. 4281-4293, 2018.

[4] C. Camposeco-Negrete, "Optimization of cutting parameters for minimizing energy consumption in turning of AISI 6061 T6 using Taguchi methodology and ANOVA," *Journal of Cleaner Production*, vol. 53, pp. 195-203, 2013.

[5] T. Ko and H. Kim, "Surface integrity and machineability in intermittent hard turning," *The International Journal of Advanced Manufacturing Technology*, vol. 18, pp. 168-175, 2001.

[6] H. L. Liu, X. Lv, C. Z. Huang, Z. B. Yin, B. Zou, and H. T. Zhu, "Tools optimization in efficient Intermittent cutting of 2.25 Cr1Mo0. 25V Steel," in *Advanced Materials Research*, vol. 188, pp. 469-474, 2011.

[7] H. L. Liu, X. Lv, C. Z. Huang, and H. T. Zhu, "Experimental study on intermittent turning 2.25 Cr-1Mo-0.25 V steel with coated cemented carbide tool," in *Advanced Materials Research*, vol. 500, pp. 128-133, 2012.

[8] D. Carou, E. Rubio, C. Lauro, and J. Davim, "The effect of minimum quantity lubrication in the intermittent turning of magnesium based on vibration signals," *Measurement*, vol. 94, pp. 338-343, 2016.

[9] F. Gong, J. Zhao, and J. Pang, "Evolution of cutting forces and tool failure mechanisms in intermittent turning of hardened steel with ceramic tool," *The International Journal of Advanced Manufacturing Technology*, vol. 89, pp. 1603-1613, 2017.

[10] X. Cui, J. Guo, and J. Zheng, "Optimization of geometry parameters for ceramic cutting tools in intermittent turning of hardened steel," *Materials & Design*, vol. 92, pp. 424-437, 2016.

[11] E. Kudryashov, I. Smirnov, E. Yatsun, and N. Khizhnyak, "Stabilizing tool for intermittent turning of complex surfaces," *Russian Engineering Research*, vol. 39, pp. 141-146, 2019.

[12] M. Nayak, R. Sehgal, and R. Kumar, "Investigating machinability of AISI D6 tool steel using CBN tools during hard turning," *Materials Today: Proceedings*, vol. 47, pp. 3960-3965, 2021.

[13] M. Yallese, J. Rigal, K. Chaoui, and L. Boulanouar, "The effects of cutting conditions on mixed ceramic and cubic boron nitride tool wear and on surface roughness during machining of X200Cr12 steel (60 HRC)," *Proceedings of the Institution of Mechanical Engineers, Part B: Journal of Engineering Manufacture*, vol. 219, no. 1, pp. 35-55, 2005.

[14] H. Bouchelaghem, M. Yallese, T. Mabrouki, A. Amirat, and J. F. Rigal, "Experimental investigation and performance analyses of CBN insert in hard turning of cold work tool steel (D3)," *Machining Science and Technology*, vol. 14, no. 4, pp. 471-501, 2010.

[15] M. Nouioua, M. A. Yallese, R. Khettabi, S. Belhadi, and T. Mabrouki, "Comparative assessment of cooling conditions, including MQL technology on machining factors in an environmentally friendly approach," *The International Journal of Advanced Manufacturing Technology*, vol. 91, pp. 3079-3094, 2017.

[16] V. Shinge and M. Pable, "Effect of nano-minimum quantity lubrication on cutting temperature and surface roughness of milling AISI D3 tool steel," *Materials Today: Proceedings*, vol. 72, pp. 1758-1764, 2023.

[17] K. Safi, M. A. Yallese, S. Belhadi, S. Boutabba, and T. Mabrouki, "Optimisation multi-objective des paramètres de coupe lors de l'usinage d'un acier pour travail à froid avec un carbure revêtu CVD (Al2O3/TiC/TiCN)," *UPB Scientific Bulletin, Series D: Mechanical Engineering*, vol. 83, no. 1, pp. 149-168, 2021.

[18] M. Uzun, Ü. A. Usca, M. Kuntoğlu, and M. K. Gupta, "Influence of tool path strategies on machining time, tool wear, and surface roughness during milling of AISI X210Cr12 steel," *The International Journal of Advanced Manufacturing Technology*, vol. 119, no. 3-4, pp. 2709-2720, 2022.

[19] A. M. M. Ibrahim, M. A. Omer, S. R. Das, W. Li, M. S. Alsoufi, and A. Elsheikh, "Evaluating the effect of minimum quantity lubrication during hard turning of AISI D3 steel using vegetable oil enriched with nano-additives," *Alexandria Engineering Journal*, vol. 61, no. 12, pp. 10925-10938, 2022.

[20] A. Naghashzadeh, A. Shafyei, and F. Sourani, "Nanoindentation and tribological behavior of TiN-TiCN-TiAlN multilayer coatings on AISI D3 tool steel," *Journal of Materials Engineering and Performance*, vol. 31, no. 6, pp. 4335-4342, 2022.

[21] D. K. Mohanta, B. Sahoo, and A. M. Mohanty, "Optimization of process parameter in AI7075 turning using grey relational desirability function and metaheuristics," *Materials and Manufacturing Processes*, pp. 1-11, 2023.

[22] S. K. Kar, P. K. Mishra, A. K. Sahu, S. S. Mahapatra, and J. Thomas, "Multi-objective optimization of wire-EDM of Inconel 625 by using desirability function approach," *International Journal on Interactive Design and Manufacturing (IJIDeM)*, pp. 1-8, 2023.

[23] A. Zerti, M. A. Yallese, O. Zerti, M. Nouioua, and R. Khettabi, "Prediction of machining performance using RSM and ANN models in hard turning of martensitic stainless steel AISI 420," *Proceedings of the Institution of Mechanical Engineers, Part C: Journal of Mechanical Engineering Science*, vol. 233, no. 13, pp. 4439-4462, 2019.

[24] S. Chihaoui, M. A. Yallese, S. Belhadi, A. Belbah, K. Safi, and A. Haddad, "Coated CBN cutting tool performance in green turning of gray cast iron EN-GJL-250: modeling and optimization," *The International Journal of Advanced Manufacturing Technology*, vol. 113, pp. 3643-3665, 2021.

[25] K. Safi, M. A. Yallese, S. Belhadi, T. Mabrouki, and S. Chihaoui, "Parametric study and multi-criteria optimization during turning of X210Cr12 steel using the desirability function and hybrid Taguchi-WASPAS method," *Proceedings of the Institution of Mechanical Engineers, Part C: Journal of Mechanical Engineering Science*, vol. 236, no. 15, pp. 8401-8420, 2022.

[26] A. H. Jawad, U. K. Sahu, N. A. Jani, Z. A. ALOthman, and L. D. Wilson, "Magnetic crosslinked chitosan-tripolyphosphate/MgO/Fe3O4 nanocomposite for reactive blue 19 dye removal: Optimization using desirability function approach," *Surfaces and Interfaces*, vol. 28, p. 101698, 2022.

[27] J.-S. Cho, D.-H. Lee, G.-J. Seo, D.-B. Kim, and S.-J. Shin, "Optimizing the mean and variance of bead geometry in the wire+ arc additive manufacturing using a desirability function method," *The International Journal of Advanced Manufacturing Technology*, vol. 120, no. 11-12, pp. 7771-7783, 2022.

[28] A. Perec, "Desirability function analysis (DFA) in multiple responses optimization of abrasive water jet cutting process," *Reports in Mechanical Engineering*, vol. 3, no. 1, pp. 11-19, 2022.

[29] A. Hamdi and S. M. Merghache, "Application of artificial neural networks (ANN) and gray relational analysis (GRA) to modeling and optimization of the material ratio curve parameters when turning hard steel," *The International Journal of Advanced Manufacturing Technology*, pp. 1-14, 2023.

[30] A. Venkata Vishnu and S. Sudhakar Babu, "Mathematical modeling & multi response optimization for improving machinability of alloy steel using RSM, GRA and Jaya algorithm," *International Journal of Engineering*, vol. 34, no. 9, pp. 2157-2166, 2021.

[31] P. Wu, Y. He, Y. Li, J. He, X. Liu, and Y. Wang, "Multi-objective optimisation of machining process parameters using deep learning-based data-driven genetic algorithm and TOPSIS," *Journal of Manufacturing Systems*, vol. 64, pp. 40-52, 2022.

[32] R. R. Panigrahi, A. Panda, A. K. Sahoo, R. Kumar, and R. R. Mishra, "Turning performance analysis and optimization of processing parameters using GRA-PSO approach in sustainable manufacturing," *Proceedings of the Institution of Mechanical Engineers, Part E: Journal of Process Mechanical Engineering*, vol. 236, no. 6, pp. 2404-2419, 2022.

[33] A. Venkata Vishnu, S. S. Babu, and P. J. Kumar, "Multi-response optimization of machining characteristics using MQL through GRA and TOPSIS approach," in *Sustainable Machining Strategies for Better Performance: Select Proceedings of SMSBP 2020*, 2022, pp. 23-37, 2022.

[34] V. R. Balwan, B. Dabade, and B. B. Kabnure, "Optimization of surface finish and material removal rate while turning hardened EN 353 steel using GRA," *Materials Today: Proceedings*, vol. 59, pp. 331-338, 2022.

[35] K. Safi, M. A. Yallese, S. Belhadi, T. Mabrouki, and A. Laouissi, "Tool wear, 3D surface topography, and comparative analysis of GRA, MOORA, DEAR, and WASPAS optimization techniques in turning of cold work tool steel," *The International Journal of Advanced Manufacturing Technology*, vol. 121, no. 1-2, pp. 701-721, 2022.

[36] M. Trifunović, M. Madić, P. Janković, D. Rodić, and M. Gostimirović, "Investigation of cutting and specific cutting energy in turning of POM-C using a PCD tool: Analysis and some optimization aspects," *Journal of Cleaner Production*, vol. 303, p. 127043, 2021.

[37] S. Y. Martowibowo, I. Ariza, and B. Damanik, "Comparison of metal removal rate and surface roughness optimization for AISI 316L using sunflower oil minimum quantity lubrication and dry turning processes," *Journal of Mechanical Engineering and Sciences*, vol. 16, no. 3, pp. 8976-8986, 2022.

[38] A. Hamza, K. Bousnina, and N. B. Yahia, "An approach to the influence of the machining process on power consumption and surface quality during the milling of 304L austenitic stainless steel," *Journal of Mechanical Engineering and Sciences*, vol. 16, no. 3, pp. 9093-9109, 2022.

[39] D. Carou, E. Rubio, C. Lauro, and J. Davim, "Experimental investigation on surface finish during intermittent turning of UNS M11917 magnesium alloy under dry and near dry machining conditions," *Measurement*, vol. 56, pp. 136-154, 2014.

[40] X. B. Cui, J. Zhao, Y. H. Zhou, and Z. Pei, "Cutting forces and tool wear in intermittent turning processes with $Al_2O_3$-based ceramic tools," in *Key Engineering Materials*, vol. 499, pp. 205-210, 2012.

[41] X. Ni, J. Zhao, F. Wang, F. Gong, X. Zhong, and H. Tao, "Failure analysis of ceramic tool in intermittent turning of hardened steel," *Proceedings of the Institution of Mechanical Engineers, Part B: Journal of Engineering Manufacture*, vol. 232, no. 12, pp. 2140-2153, 2018.

[42] U. M. R. Paturi, A. Yash, S. T. Palakurthy, and N. Reddy, "Modeling and optimization of machining parameters for minimizing surface roughness and tool wear during AISI 52100 steel dry turning," *Materials Today: Proceedings*, vol. 50, pp. 1164-1172, 2022.

[43] B. Eskandari, S. Bhowmick, and A. T. Alpas, "Turning of Inconel 718 using liquid nitrogen: multi-objective optimization of cutting parameters using RSM," *The International Journal of Advanced Manufacturing Technology*, vol. 120, no. 5-6, pp. 3077-3101, 2022.

[44] P. Anggoro, Y. Purharyono, A. A. Anthony, M. Tauviqirrahman, and A. Bayuseno, "Optimisation of cutting parameters of new material orthotic insole using a Taguchi and response surface methodology approach," *Alexandria Engineering Journal*, vol. 61, no. 5, pp. 3613-3632, 2022.

[45] S. A. Bagaber and A. R. Yusoff, "Multi-objective optimization of cutting parameters to minimize power consumption in dry turning of stainless steel 316," *Journal of cleaner production*, vol. 157, pp. 30-46, 2017.

[46] O. Benkhelifa, A. Cherfia, and M. Nouioua, "Modeling and multi-response optimization of cutting parameters in turning of AISI 316L using RSM and desirability function approach," *The International Journal of Advanced Manufacturing Technology*, vol. 122, no. 3-4, pp. 1987-2002, 2022.

[47] Ü. A. Usca *et al.*, "Tool wear, surface roughness, cutting temperature and chips morphology evaluation of Al/TiN coated carbide cutting tools in milling of Cu–B–CrC based ceramic matrix composites," *Journal of Materials Research and Technology*, vol. 16, pp. 1243-1259, 2022.

[48] A. T. Abbas, A. A. Al-Abduljabbar, I. A. Alnaser, M. F. Aly, I. H. Abdelgaliel, and A. Elkaseer, "A closer look at precision hard turning of AISI4340: multi-objective optimization for simultaneous low surface roughness and high productivity," *Materials*, vol. 15, no. 6, p. 2106, 2022.

[49] D. R. Shah, N. Pancholi, H. Gajera, and B. Patel, "Investigation of cutting temperature, cutting force and surface roughness using multi-objective optimization for turning of Ti-6Al-4 V (ELI)," *Materials today: proceedings*, vol. 50, pp. 1379-1388, 2022.

[50] B. Li, X. Tian, and M. Zhang, "Modeling and multi-objective optimization method of machine tool energy consumption considering tool wear," *International Journal of Precision Engineering and Manufacturing-Green Technology*, vol. 9, pp. 127-141, 2022.

[51] S. P. Anand and A. K. Saraf, "Optimization of surface roughness and material removal rate in turning of AISI D3 steel with coated carbide inserts," in *IOP Conference Series: Materials Science and Engineering*, vol. 1224, no. 1, p. 012010, 2022.

[52] A. El-Araby, I. Sabry, and A. El-Assal, "A comparative study of using MCDM methods integrated with entropy weight method for evaluating facility location problem," *Operational Research in Engineering Sciences: Theory and Applications*, vol. 5, no. 1, pp. 121-138, 2022.

[53] D. Mukherjee, R. Ranjan, and S. Moi, "Multi-response optimization of surface roughness and MRR in turning using Taguchi Grey Relational Analysis (TGRA)," *International Research Journal of Multidisciplinary Scope (IRJMS)*, vol. 3, pp. 1-7, 2022.